

Autofluorescence of pigmented skin lesions using a pulsed UV laser

Cheng, Haynes P. H.; Svenmarker, Pontus; Xie, Haiyan; Tidemand-Lichtenberg, Peter; Jensen, Ole B.; Bendsöe, Niels; Svanberg, Katarina; Petersen, Paul Michael; Pedersen, Christian; Andersson-Engels, Stefan; Andersen, Peter E.

Published in:

Proceedings of SPIE

10.1117/12.855837

2010

Link to publication

Citation for published version (APA): Cheng, H. P. H., Svenmarker, P., Xie, H., Tidemand-Lichtenberg, P., Jensen, O. B., Bendsöe, N., Svanberg, K., Petersen, P. M., Pedersen, C., Andersson-Engels, S., & Andersen, P. E. (2010). Autofluorescence of pigmented skin lesions using a pulsed UV laser. In *Proceedings of SPIE* (Vol. 7715, pp. 77151K-1). SPIE. https://doi.org/10.1117/12.855837

Total number of authors:

Unless other specific re-use rights are stated the following general rights apply: Copyright and moral rights for the publications made accessible in the public portal are retained by the authors and/or other copyright owners and it is a condition of accessing publications that users recognise and abide by the legal requirements associated with these rights.

• Users may download and print one copy of any publication from the public portal for the purpose of private study

- You may not further distribute the material or use it for any profit-making activity or commercial gain
 You may freely distribute the URL identifying the publication in the public portal

Read more about Creative commons licenses: https://creativecommons.org/licenses/

Take down policy If you believe that this document breaches copyright please contact us providing details, and we will remove access to the work immediately and investigate your claim.

Download date: 17. Dec. 2025

Autofluorescence of pigmented skin lesions using a pulsed UV laser with synchronized detection: clinical results

Haynes P. H. Cheng*a, Pontus Svenmarkerb, Haiyan Xieb, Peter Tidemand-Lichtenberga, Ole B. Jensena, Niels Bendsoec, Katarina Svanbergd, Paul Michael Petersena, Christian Pedersena, Stefan Andersson-Engelsb, Peter E. Andersena

^a DTU Fotonik, Frederiksborgvej 399, DK-4000, Roskilde, Denmark;
 ^b Department of Physics, Lund University, P.O. Box 118, SE-22100, Lund, Sweden;
 ^c Department of Dermatology and Venereology, Lund University Hospital, SE-22185, Lund, Sweden;
 ^d Department of Oncology, Lund University Hospital, SE-22185, Lund, Sweden

ABSTRACT

We report preliminary clinical results of autofluorescence imaging of malignant and benign skin lesions, using pulsed 355 nm laser excitation with synchronized detection. The novel synchronized detection system allows high signal-to-noise ratio to be achieved in the resulting autofluorescence signal, which may in turn produce high contrast images that improve diagnosis, even in the presence of ambient room light. The synchronized set-up utilizes a compact, diode pumped, pulsed UV laser at 355 nm which is coupled to a CCD camera and a liquid crystal tunable filter. The excitation and image capture is sampled at 5 kHz and the resulting autofluorescence is captured with the liquid crystal filter cycling through seven wavelengths between 420 nm and 580 nm. The clinical study targets pigmented skin lesions and evaluates the prospects of using autofluorescence as a possible means in differentiating malignant and benign skin tumors. Up to now, sixteen patients have participated in the clinical study. The autofluorescence images, averaged over the exposure time of one second, will be presented along with histopathological results. Initial survey of the images show good contrast and diagnostic results show promising agreement based on the histopathological results.

Keywords: autofluorescence imaging, photodynamic therapy, skin lesion, diagnostic

1. INTRODUCTION

Fluorescence imaging provides a powerful diagnostic tool in monitoring treatment progress in photodynamic therapy (PDT) and in differentiating between malignant and benign lesions non-invasively prior to treatment. The technique is relatively economical, non-invasive, and provides information in real-time. While exogenous fluorophores exist, they generally require uptake of the photosensitizer, and the patient may need to avoid exposure to light for a period of time before and after the procedure. By taking advantage of endogenous fluorophores, autofluorescence imaging is a promising diagnostic tool for differentiating between different types of pigmented skin lesions without prior preparation on the patient.

While the specific endogenous agents responsible for the fluorescence signal are not fully understood thus far, it has been suggested that it could be due to collagen cross-links, elastin, NADH, and/or keratin [1]. Using a high pressure mercury lamp in combination with a bandpass filter at 366 nm, Lohmann *et al.* reported a fluorescence peak at 475 nm and a possible shoulder at 445 nm, which may be attributed to the fluorescence peak of NADH and NAD respectively [2]. Lohmann *et al.* suggested that relative fluorescence intensities between healthy skin and the lesion area could be used to differentiate between a mole and a melanoma. Using a high pressure Xe-Hg lamp, and an algorithm based on that proposed by Lohmann *et al.*, Chwirot *et al.* reported a clinical study achieving 82.7% sensitivity and 59.9% specificity for detecting melanomas in dark room conditions [1]. Troyanova *et al.* presented autofluorescence spectra of benign and dysplastic nevi and malignant melanoma using a nitrogen laser at 337 nm [3]. In a separate publication, Borisova *et al.* reported on autofluorescence spectra of basal cell carcinoma (BCC), squamous cell

*hach@fotonik.dtu.dk

Biophotonics: Photonic Solutions for Better Health Care II, edited by Jürgen Popp, Wolfgang Drexler, Valery V. Tuchin, Dennis L. Matthews, Proc. of SPIE Vol. 7715, 77151K © 2010 SPIE · CCC code: 1605-7422/10/\$18 · doi: 10.1117/12.855837

carcinoma (SCC), keratoacanthoma, and benign skin lesions using LED's at various wavelengths as excitation light source [4].

In this paper, a synchronized detection system has been put together using a compact, diode-pumped UV laser at 355 nm and a tunable liquid crystal filter with gated detection to increase the signal-to-background ratio to the extent that imaging in ambient room light is possible. This study targets pigmented skin lesions because of the difficulty associated with their classification without the use of histopathological analysis. Sixteen patients have participated in the clinical studies and the resulting autofluorescence images, as well as the corresponding histopathological results are presented.

2. METHODOLOGY

2.1 Apparatus

The synchronized detection system is described below and is illustrated in the block diagram in Fig. 1. The pulsed UV laser at 355 nm delivers Gaussian-shaped pulses of 10 ns duration FWHM at a repetition rate of 5 kHz through a 50 m long multimode fibre, which also serves as an optical delay line that accommodates the response time of the electronics involved. Shutter 2 acts as the detection gate and is triggered by residual 1064 nm light (also at 5 kHz) that is coupled out through a separate port in the laser. The 1064 nm optical pulse train is converted into an electronic signal by a fast photodiode, which then goes to an electronic delay circuit that is used to fine-tune the temporal overlap between the UV light pulse and the shutter trigger signal during system calibration.

The images are captured using a CCD camera (iSTAR DH734-18F-75) that comes with a proprietary PCI analog-to-digital (ADC) converter. The iSTAR CCD has an integrated optical intensifier on the front side, denoted as shutter 2 in Fig. 1, that is controlled by the ADC and acts as the detection gate. Thus, the 5 kHz repetition rate is limited by the response time of shutter 2. An external mechanical shutter, shutter 1 in Fig. 1, is used to control the exposure time of each image taken, which is set to one second during the clinical trial. The iSTAR ADC has an input port, used in this case to obtain the trigger signal from the photodiode, and an output port used to control shutter 1. The tunable filter used is a VariSpec VIS from CRi with a bandwidth of 20 nm, and a tuning range from 400 nm to 720 nm, and is connected to a computer, which cycles through the pass-band wavelengths of the filter after an image has been taken (i.e. after shutter 1 has been opened and closed.)

Fluorescence images are taken at seven wavelengths: at 420 nm, 440 nm, 460 nm, 480 nm, 500 nm, 560 nm and 580 nm. An exposure time of one second for each fluorescence image corresponds to integrating over approximately 5000 frames for each image, with each frame being illuminated with a 10 ns FWHM Gaussian-shaped light pulse.

The target is imaged onto the CCD using an off-the-shelf 50 mm F/1.4 camera lens.

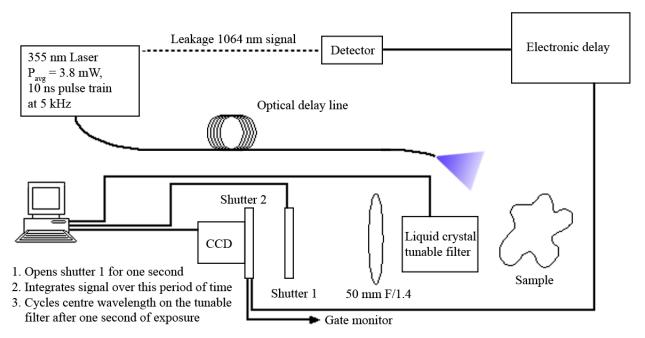


Figure 1. Block diagram of system setup with synchronized detection

A mechanical mount, housing the fibre output, shutters, liquid crystal filter, and CCD camera, was built to aid in stabilizing the light source and CCD camera during image acquisition.

2.2 Pulsed UV Laser

The UV laser is a diode-pumped Nd:YAG 1064 nm laser, frequency-tripled to 355 nm. Its schematic diagram is illustrated in Fig. 2. The pump diode (RPMC LDX-3415-808, LD1 in Fig. 2) produces 4 W of optical power at 808 nm when pumped at a current of 3.5 A. However, it was operated at approximately 3.1 A during the clinical trials to achieve a repetition rate of 5 kHz, the maximum achievable with the optical intensifier being used as the detection gate (Shutter 2 in Fig. 1).

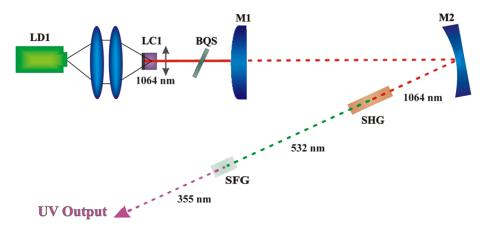


Figure 2. Schematic diagram of the pulsed UV Laser used

The 5 mm long Nd:YAG crystal is placed in a 30 mm long optical resonator with a Brewster-cut Cr:YAG saturable absorber that gives 20% small signal absorption. Transmission of the output coupler (M1 in Fig. 2) is 80% at 1064 nm. This gives approximately 121 mW of average power at 1064 nm at a pump current of 3.1 A, corresponding to 2.5 kW of peak power at 1064 nm. The laser beam is then focused into a PPKTP and a BBO crystal for the second-harmonic generation and third-harmonic mixing respectively. Mirror M2, with a curvature of 75 mm, was used such that a beam waist of approximately 100 µm is formed at the midpoint between the two crystals, placed approximately 20 mm apart.

The PPKTP crystal is temperature-tuned so that approximately half of the 1064 nm light is converted into its second-harmonic at 532 nm. After sum frequency mixing in the BBO crystal between the residual 1064 nm and the generated 532 nm power, an average power of 3.8 mW at 355 nm was achieved, corresponding to a peak power of 76 W. Coupling losses and attenuation associated with the optical fibre has not been measured during this clinical trial, but it is observed that sufficient UV light is produced for image capture.

2.3 Calibration

To ensure a good temporal overlap between the illumination light pulse and the opening of shutter 2, a second fast photodiode (Melles Griot 13DAH001), with a rise time of less than 1 ns, is placed at the output of the optical fibre to monitor arrival of the UV pulses. The electronic delay is then adjusted, which in turn controls the timing of shutter 2. The photodiode signal is monitored on an oscilloscope, while the state of shutter 2 is monitored through a gate monitor signal from the proprietary PCI board that came with the iSTAR CCD camera. Shutter 2 is configured to remain open for 30 ns after it has been triggered, and the electronic delay is adjusted such that the peak of the UV pulse arrives 15 ns after the shutter is opened. The Melles Griot photodiode is only used during calibration and is not used during normal operation of the laser.

2.4 Post-processing

To obtain consistent fluorescence signals with different scattering properties across different patients and to increase sensitivity, the fluorescence images are presented as a ratio of the fluorescence images at different wavelengths. Specifically, the fluorescence image at 580 nm is divided by the image at 460 nm, and a second ratioed image is produced using the signal at 440 nm divided by the signal at 500 nm. This in effect probes the fluorescence spectra of the different types of lesions at the four wavelengths. In principle, since fluorescence images at 7 wavelengths were captured, 28 combinations are possible. In this preliminary presentation, the mentioned wavelengths are chosen as they seem to provide the best contrast. Furthermore, to suppress the effects of hot pixels, the ratioed images are plotted in a log scale, in dB, using false colors.

3. RESULTS

By integrating over approximately 5000 frames per fluorescence image, sufficient signal could be collected in ambient room light to produce the ratioed images. Preliminary results show good contrast in six patients, while images from another six patients were not of good quality due to movement of the patient, out of focus, or hard-to-access areas, and four images showed poor contrast, which may be attributed to insufficient excitation light. Table 1 shows the patient data (age, sex, location of tumour and the corresponding histopathological diagnosis), while Fig. 3 shows the corresponding autofluorescence images.

TC 11 1	D 4 1 4	1 2/1	1' 1' /	41 1 1 14
Table I	Patient data :	aiong with corresn	onaing histor	nathological results

	Age	Sex	Location of tumour	Histopathological Diagnosis
Patient 1	89	M	Trunk (right side)	Squamous cell carcinoma in situ
Patient 3	76	F	Lower left leg	Malignant melanoma
Patient 8	36	M	Trunk (back)	Benign nevus
Patient 12	85	F	Trunk (back)	Basal cell carcinoma
Patient 14	42	F	Left arm	Junction nevus with displasia
Patient 15	36	M	Trunk (left side)	Hemangioma

The first column in Fig 3. shows the grayscale images captured using white light illumination without any spectral filtering. The second column is the ratioed fluorescence images of 580 nm/ 460 nm, where the color-bars show the scale in dB. The third column is the ratioed fluorescence images of 440 nm/ 500 nm, where the color-bars show the scale in dB. The fourth column shows the raw fluorescence images at 480 nm, corresponding to the fluorescence peak of NADH.

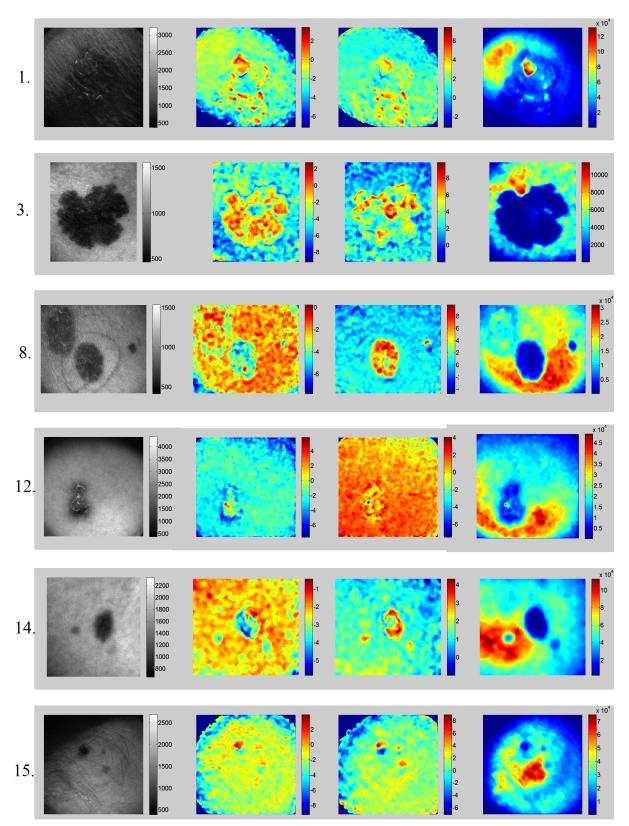


Figure 3. Autofluorescence images of pigmented skin lesions.

It could be seen that in patient 8 and patient 14, the contrast in the ratioed images were particularly strong, which may be due to the stronger fluorescence response in nevi when compared to melanoma, as previously reported in [3]. The ratioed signal from the nevi is slightly stronger than that coming from the surrounding tissue, which is true for both the 440 nm and 460 nm fluorescence. On the other hand, it could be seen that the non-ratioed fluorescence signal from the melanoma in patient 3 is particularly low at 480 nm, which is inline with fluorescence spectrum previously reported in [2] and [3].

While previous reports on the emission spectrum of benign, malignant and normal skin tissue [3] suggest fluorescence signals between 430 nm and 450 nm may be of interest in detecting the NADH, NAD fluorescence contrast, thereby aiding in the differentiation between these types of tissue, the transmission of the liquid crystal filter is relatively low at the these wavelengths, ranging from 8% at 420 nm to 20% at 460 nm. Therefore, a higher transmission filter may be better able to produce higher contrast in the ratioed fluorescence images. Moreover, a higher power light source would allow shorter exposure times, reducing the blurring effects due to movement during image acquisition. Nonetheless, even with these deficiencies, the preliminary images show promising results.

4. CONCLUSION

In conclusion, preliminary results from the clinical study on pigmented skin lesions have been presented. Autofluorescence images were obtained using a pulsed excitation light source at 355 nm and a synchronized and gated imaging system. This allowed for better signal-to-background ratio, to the extent that imaging in ambient room light is possible. The preliminary images from the clinical study show good contrast; however, further investigation into the optimal ratioing wavelengths with a larger sample set may be beneficial. Furthermore, filters with higher transmittance at the low detection wavelengths can be integrated into the system to further evaluate the feasibility of autofluorescence diagnostic of pigmented skin lesions.

ACKNOWLEDGEMENT

The authors acknowledge the financial support of the European Community through the FP-6 project WWW.BRIGHTER.EU contract IST-2005-035266.

REFERENCES

- [1] Chwirot, B.W., Chwirot, S., Sypniewska, N., Michniewicz, Z., Redzinski, J., Kurzawski, G. and Ruka, W., "Fluorescence In Situ Detection of Human Cutaneous Melanoma: Study of Diagnostic Parameters of the Method," Journal of Investigative Dermatology, 117(6), 1449-1451 (2001).
- [2] Lohmann, W. and Paul, E., "In situ Detection of Melanomas by Fluorescence Measurements," Naturwissenschaften, 75, 201-202 (1988).
- [3] Troyanova, P., Borisova, E., Stoyanova, V. and Avramov, L., "Laser-induced autofluorescence spectroscopy of benign and dysplastic nevi and malignant melanoma," Proc. SPIE 6284, 62840K (2006).
- [4] Borisova, E., Dogandjiiska, E., Bliznakova, I., Avramov, L., Pavlova, E. and Troyanova, P., "Multispectral autofluorescence diagnosis of non-melanoma cutaneous tumors," Proc. of SPIE-OSA Biomedical Optics, SPIE Vol. 7368, 736823 (2009).